

# Biocorrosion on Surface of ASTM A283 Carbon Steel, Exposed in Diesel S10 and Tap Water

Diana Magalhães Frazão<sup>a\*</sup>, Ivanilda Ramos de Melo<sup>a</sup>, Maxime Montoya<sup>a</sup>,

Severino Leopoldino Urtiga Filho<sup>a</sup>

<sup>a</sup>Departamento de Engenharia Mecânica, Universidade Federal de Pernambuco, Recife, PE, Brazil

Received: January 17, 2017; Revised: December 08, 2017; Accepted: December 11, 2017

This paper sets out to evaluate the corrosion and biocorrosion of carbon steel ASTM A283 exposed to a Diesel S10 oil/tap water system under static conditions for 90 days. The following analyzes were performed: physico-chemical in tap water, sulfur content in Diesel S10 and quantification of sessile microorganisms in the biofilm formed on the metal. To monitor the corrosion process, mass loss, scanning electron microscopy (SEM), energy dispersive spectroscopy (EDS), confocal laser microscopy and X-ray diffraction (XRD) were performed. There were changes in the composition of the medium, correlated with the formation of corrosion and biofilm products. There was biodegradation of the fuel, which in contact with water influenced the development of microorganisms. Moreover, the corrosion rate was classified as moderate, the main form of corrosion being seen to be local alveolar corrosion. Therefore, the results revealed that water in diesel oil can be an aggravating factor in the process of corrosion and biocorrosion.

**Keywords:** Diesel S10, Carbon steel A283, Corrosion, Biocorrosion, Topography and Roughness.

## 1. Introduction

Corrosion is a phenomenon that occurs in iron and many ferrous alloys. This is what happens to carbon steel when exposed to the atmosphere or submerged in water. Steel is one of the materials most used in the construction of fuel distribution and storage systems. However, there are few studies on how and why corrosion occurs on metal surfaces in the presence of Diesel S10 oil contaminated with tap water<sup>1</sup>. According to the Manual Técnico da Petrobras<sup>2</sup>, Diesel S10 oil was introduced into the domestic market in January 2013. This fuel was developed to meet the requirements of the newest generation of diesel engines which were designed to emit less particulate (PM) and nitrogen oxides (NO<sub>x</sub>) contents compared to those produced previously. Thus, the maximum sulfur content of the Diesel S10 oil is 10 ppm (parts per million). Therefore, it is important to investigate how corrosion behavior, which is associated with the action of the environment and chemical, physical and biological factors, occurs. In the industrial sector, biological action is of great importance, due to the activity or action of microorganisms, which can directly or indirectly influence the process of corrosion of metal surfaces<sup>3</sup>. According to the Agência Nacional de Petróleo, Gás Natural e Biocombustíveis (ANP)<sup>4</sup>, Diesel S10 has become more sensitive to being contaminated by microorganisms. It was observed that reducing the sulfur content decreased the natural bactericidal properties. Moreover, this effect would be increased with the addition of biodiesel, since it is very hygroscopic. This feature provides a higher moisture absorption and, consequently, allows microbiological action, which occurs

mainly at the fuel / water interface. This interface is an environment conducive to microbial growth, either in the presence of oxygen (aerobic) or in its absence (anaerobes)<sup>5</sup>. In view of this, the recent commercialization of Diesel S10 is of concern to the petroleum industry because of the greater possibility of contamination and / or biodegradation in fuel storage and transport tanks due to the presence of water. Such contamination can occur from the initial stage, with the production of diesel, which can be derived from the process of condensation and washing; and continue up to the final stage, when diesel is delivered to the consumer. The objective of this study was to evaluate the corrosion and biocorrosion of carbon steel ASTM A283 when exposed to a static system containing S10 Diesel oil and tap water in the ratio of 1/1 (v / v) in a 90-day timeframe.

## 2. Materials and Methods

In order to evaluate how and why corrosion and biocorrosion occurs, immersion tests were performed on four reactor systems, as shown in Fig. 1. Reactors 1, 2 and 3, corresponding to Fig. 1 (A, B, C), respectively, make up the biphasic system. They contain the same diesel / water proportions (1/1 v / v), ie 4L of water and 4L of diesel. Also there is Reactor 4 (Fig. 1 (D)), which contains 100% S10 diesel oil (8L of diesel). This 1/1 ratio was necessary to obtain an ideal volume and thus to perform all the analyses in the fluids. For the two-phase diesel / water system the immersion tests were finalized at 30, 60 and 90 days for Reactors 1, 2 and 3, respectively. For the system containing pure diesel (Reactor 4), the analyzes were performed at the end of 90

\*e-mail: [diana.lagatha@gmail.com](mailto:diana.lagatha@gmail.com)

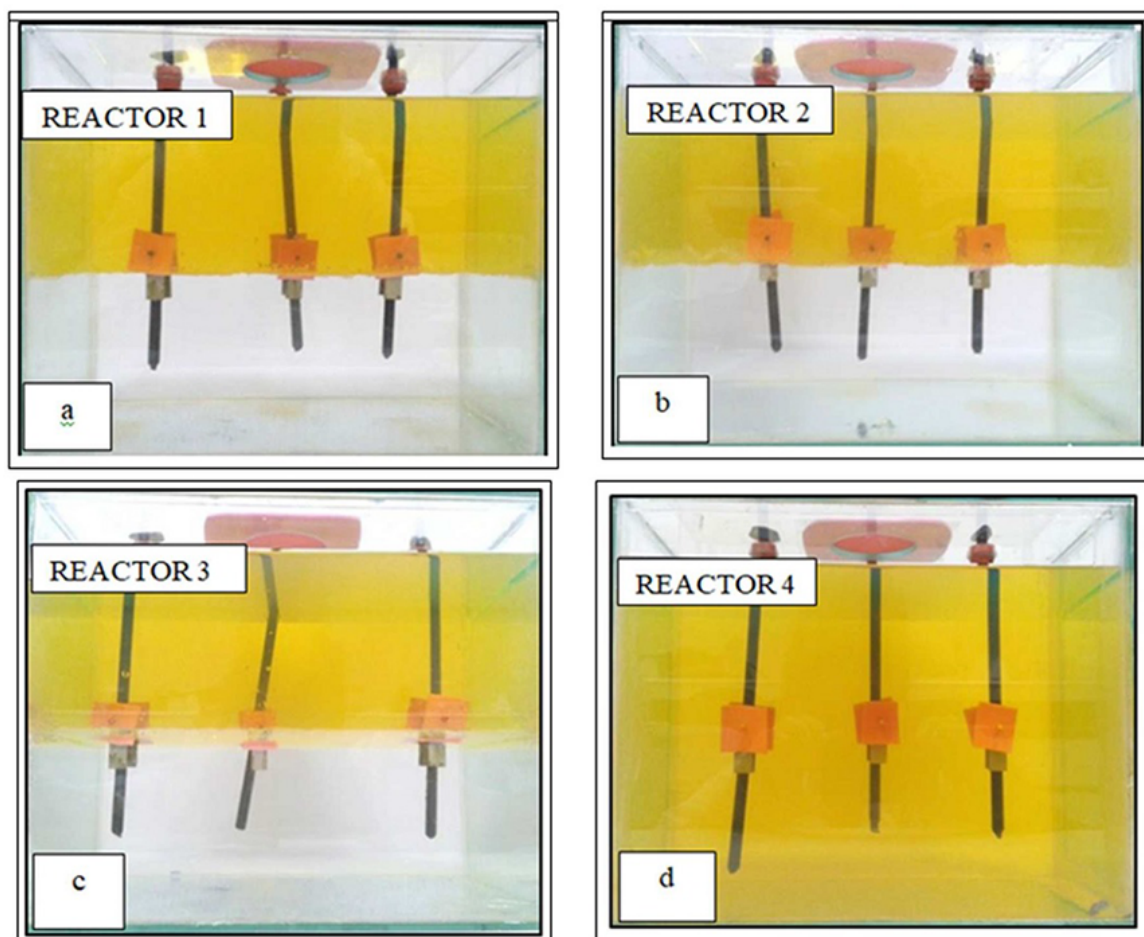


**Figure 1.** Reactors containing carbon steel A283, with 6 specimens in each reactor: (a) Reactor 1, immersion of 30 days; (b) Reactor 2, immersion of 60 days; (c) Reactor 3, immersion of 90 days and (d) Reactor 4, immersion of 90 days.

days of immersion. Each reactor contained 6 specimens, which were distributed according to the characterizations to be performed. Before the immersion process, these characterizations were obtained to analyze the images of the metallic surfaces. And they were used as standard images and compared with images obtained over 90 days.

The specimens that were exposed to S10 Diesel / tap water medium were obtained from carbon steel ASTM A283<sup>6</sup> with an elemental composition (wt%) of 0.14 C, 0.93 Mn, 0.01 Si, 0.021 P, 0.01 Cr, 0.01 Ni, 0.01 Cu, 0.042 Al, 0.001 V, 0.003 W, 0.001 Ti, 0.003 Nb and Fe equilibrium. This steel is usually used to manufacture fuel storage tanks.

The specimens were machined in the dimensions of 30 mm x 10 mm x 3 mm and a 6 mm diameter hole was drilled at one end. This equates to an exposed area of approximately 840 mm<sup>2</sup> in contact with static fluids. This hole served only to suspend the specimens in the middle (half of each specimen immersed in water and half immersed in diesel). Subsequently, the specimens were sandblasted with glass microspheres to homogenize their roughness and favor a better adhesion of the biofilm and corrosion products. Before being immersed,

they also underwent a cleaning or degreasing process, during which they spent 5s in isopropyl alcohol and 5s in acetone, in accordance with Standard ASTM G1-03<sup>7</sup>.

In order to obtain the mass loss as a function of the initial and final mass, the specimens underwent the mass measurement process before and after each immersion time (30, 60, 90 days), with a high precision balance (0.1 mg resolution). Out of the 6 specimens, 3 were removed from each reactor, in its specific time, with the aid of a sterile forceps. They were placed in containers containing 30 mL of reducing solution. Subsequently, mechanical scraping was performed with the aid of tweezers and a sterile spatula. Thus, the entire area of each specimen was aseptically scraped in order to totally remove biofilms which had formed on their surface. The biofilm was removed and packed in the sterile containers and was used for microbiological quantification. After mechanical scraping, each specimen was transferred to a Petri dish and submitted to acid pickling, for which it remained in the acid solution for 10 seconds, and was then placed in isopropyl alcohol and finally in acetone. The specimens were transferred to a desiccator and kept under

vacuum for 5 minutes. After 24h, they were weighed to the tenth of a thousandth of a gram in order to investigate the variation of the mass to obtain the corrosion rate according to the Standard ASTM G1-03<sup>7</sup> as per Equation 1:

$$\text{Corrosion Rate} = \frac{(KxW)}{(AxTxD)} \quad (1)$$

where:

- K is a constant of value equal to  $8.76 \times 10^4$  mm / year;
- T is the exposure time in hours;
- A is the area of the metal part in  $\text{cm}^2$ ;
- W is the mass loss in grams (initial weight - final weight);
- D is the density of A283 steel, approximately 7.86 g /  $\text{cm}^3$ .

In order to evaluate the loss of mass of the carbon steel test specimens, Standard NACE RP-0775<sup>8</sup> was adopted, which establishes the levels of corrosivity for carbon steel. These three specimens, whose products were removed from their surfaces, were not only used to obtain the corrosion rate and to perform the microbial quantification in the biofilm, but also to analyze the SEM / EDS, topography and roughness. These analyses were performed on the surface of the metal immersed in water and on the surface of the metal immersed in oil.

In order to fix the biofilm and the corrosion products on the metal surface, the 3 remaining specimens which were used to analyze SEM and XRD on the ASTM A283 carbon steel surface were immersed in 5% glutaraldehyde solution in cacodylate for 24 hours. Subsequently, to finish the fixation process, they were each submitted to 3 10-minute baths, in 0.1M cacodylate, to be dehydrated in ethyl alcohol, in proportions of 30 to 100%, in each of which they remained for 5 minutes<sup>9</sup>. Finally, they were placed on Petri dishes and in a vacuum desiccator for 5 minutes. Of these three specimens only 1 was used for SEM analysis after biofilm fixation, and it was metalized with gold (15 nm thickness).

The physicochemical analyses were performed in tap water. The parameters analyzed were chloride ions, total iron and sulfate ions according to Methods APHA 4110<sup>10</sup> and 3120<sup>11</sup>. These tests were performed before immersion and after 90 days.

In order to obtain information on the biodegradation of the fuel, an analysis of the sulfur content in the diesel oil S10 was carried out. This analysis followed Standard ASTM D 5453<sup>12</sup> - the Standard Test Method for Determining Total Sulfur in Light Hydrocarbons, Spark Ignition Engine Fuel, Diesel Engine Fuel and Engine Oil by Ultraviolet Fluorescence (ANP) Motor Oil, No. 50 on 23.12. 2013 - DOU 24.12.2013<sup>12</sup>.

Quantifying the main sessile microbial groups was performed on the biofilm which had adhered to the metal: total aerobic bacteria, acid-producing aerobic bacteria,

iron- precipitating bacteria, total anaerobic bacteria and acid-producing anaerobic bacteria.

The following is the production of the diluents for aerobic and anaerobic culture media. The aerobic microorganisms were quantified by diluting them in saline solution of 0.85% NaCl, while the anaerobes were quantified in the reducing solution.

Total aerobic bacteria were quantified by counting Colony Forming Units (CFU) in a dehydrated Plate Count Agar (PCA) culture medium (Merck, Darmstadt, Germany) using the Pour Plate technique after 48 hours of incubation at  $35 \pm 1$  °C. The pH was adjusted to  $7.0 \pm 0.2$ .

Anaerobic and aerobic acid producing bacteria were quantified using the Most Probable Number (MPN) technique in red dehydrated phenol broth medium (Himedia, Mumbai, India), supplemented with 1% sucrose, after 48 hours of incubation at  $35 \pm 1$  °C. After homogenization, the pH was adjusted to  $7.4 \pm 0.2$ . For anaerobic bacteria only, the medium was purged with  $\text{N}_2$  for 20 minutes.

The iron precipitating bacteria were quantified using the Pour Plate technique in medium containing ammoniacal ferric citrate after 15 days of incubation at  $35 \pm 1$  °C. After homogenization, the pH was adjusted to  $6.6 \pm 0.1$ . This medium was stored without being exposed to light.

Total anaerobic bacteria were quantified using the Most Probable Number (MPN) technique, in a sodium thioglycolate fluid medium (Himedia, Mumbai, India) purged with  $\text{N}_2$ , after 21 days of incubation at  $35 \pm 1$  °C. After complete homogenization, the pH was adjusted to  $7.1 \pm 0.2$ . The tubes were stored at room temperature.

All media were autoclaved at a pressure of 1 atm and a temperature of 121 °C for 15 minutes. After removing the culture media from the autoclave, it was necessary to stir them for complete homogenization and, finally, they were stored at room temperature.

## 3. Results and Discussion

### 3.1. Corrosivity of tap water over time

Physical-chemical characterization in tap water was performed to obtain the main parameters related to the corrosion process. It was obtained at the initial time (before the experiments) and after 90 days, as shown in Table 1. As can be seen, water presented low salinity in terms of chloride and sulphate content in general.

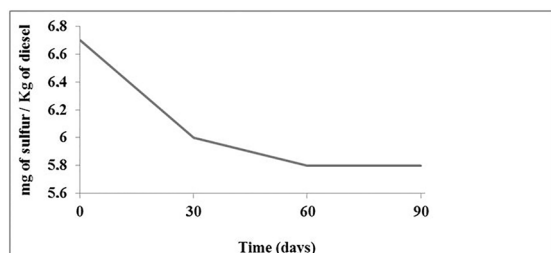
A reduction in chloride ions, from 73.95 to 24.2 mg/L, was observed between the initial state and after 90 days. This reduction is directly associated with the corrosion kinetics itself. The medium lost chloride ions due to their combining with the metal to form ferric chloride as observed by Peters et al.<sup>13</sup> Thus, over time, the corrosivity of the medium was reduced, due to the decrease in the content of chloride ions in the water.

**Table 1.** Physical-chemical results of tap water.

Parameter	Time 0	90 days
Chlorides (mg/L Cl <sup>-</sup> )	73,95	24,2
Total Iron (mg/L Fe)	<0,05	10,97
Sulfates (mg/L SO <sub>4</sub> )	7,41	25,3

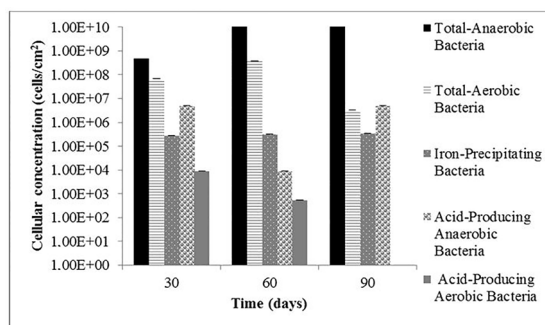
During the oxidation of the ASTM A283 carbon steel, the dissolved iron was transferred to the medium, which may explain the increase of <0.05 to 10.97 mg/L of iron in the water, as shown in Table 1. This behavior can also be explained as a result of the action of iron precipitating bacteria. They have the ability to oxidize ferrous ions (Fe<sup>2+</sup>) to ferric ions (Fe<sup>3+</sup>) as a means of obtaining energy, thereby causing the precipitation of ferric hydroxide<sup>14</sup>.

As for the sulfate content, there was also an increase from 7.41 to 25.3 mg/L. Coincidentally, there was a reduction in sulfur content in Diesel S10 oil during the experiments due to the fuel biodegrading, as shown in Fig. 2. Microorganisms may have used fuel as a source of carbon and energy as a result of the exchange of nutrients between diesel and water<sup>14</sup>. Water contains nutrients that are needed for microorganisms to develop and, in addition to carbon from hydrocarbons, they are the factors that most influence microbial growth in petroleum-derived fuels. Therefore, the consequence is the production of emulsifying agents that promote the development of microorganisms at the oil/water interface and accelerate the decomposition of the oil and its solubility in water<sup>15</sup>.

**Figure 2.** Total sulfur content in the S10 Diesel samples in contact with water.

### 3.2. The presence of sessile microorganisms in the biofilm

The quantification of the main sessile microbial groups is shown in Fig. 3. As can be seen, the quantification of total aerobic bacteria reached its maximum value,  $3.9 \times 10^8$  CFU / cm<sup>2</sup>, at 60 days, while the total anaerobic bacteria reached its maximum value,  $5 \times 10^{10}$  MPN / cm<sup>2</sup>, at 90 days. The concentration of the aerobic microorganisms decreased after 90 days, due to the system being static, without oxygen renewal. This behavior is associated with the very dynamics of biofilm formation and the synergism of microorganisms present in the medium. Over time, the thickness of the biofilm increased, which helped it separate from the sample

**Figure 3.** Quantification of sessile microorganisms in the biofilm.

and activated the dynamic process of biofilm renovation<sup>14</sup>. This also impaired the diffusion of oxygen and nutrients in the biofilm, as observed by Delaunoy et al.<sup>16</sup>, when they analyzed the biocorrosion processes in steel tubes in a water distribution system. Given the lack of oxygen, favorable conditions were provided through the microorganisms for the development and growth of anaerobic bacteria, thus characterizing a microbial consortium<sup>14</sup>. Similar results were found by Lewandowski and Boltz<sup>17</sup> in aqueous environments. The adsorption of bacteria on the surfaces formed gelatinous films from extracellular polymer substances that are excreted. These microbial activities contributed to the corrosion process on the metal surface.

### 3.3. Characterizing the corrosion

#### 3.3.1 Influence of microorganisms and corrosivity of water on corrosion rate

According to the results presented in Fig. 4a, the corrosion rate was classified as moderate up to 30 and 60 days (0.030 and 0.026 mm / year, respectively) and as low in 90 days (0.021 mm / year) for the biphasic system, in accordance with NACE-RP-0775<sup>8</sup>. For Diesel S10 oil, the corrosion rate was classified as low by 90 days (0.00026 mm / year).

As noted, the corrosion rate in the Diesel S10 oil is much lower than in the biphasic system. The surface of the sample exposed only in Diesel S10 did not show changes to the naked eye as shown in Fig. 4b (4). This result can be explained by the properties of the oil. According to Vieira<sup>18</sup>, the oil is characterized as having low conductivity and high resistivity. These factors contribute to the low ion exchange between the medium and the metal surface. This tends to reduce the rate of corrosion. However, this does not mean that corrosion on the metal surface cannot occur in the presence of diesel oil. It is necessary to take into account the fact that automotive diesel oil consists of a mixture of biodiesel and diesel oil. Moreover, the predominant characteristic of biodiesel is to be quite hygroscopic, that is, it has a propensity to absorb water. In addition, biodiesel is biodegradable, due to the action of microorganisms, which favor a lower oxidative stability, thus reducing the useful life of the fuel. Therefore,

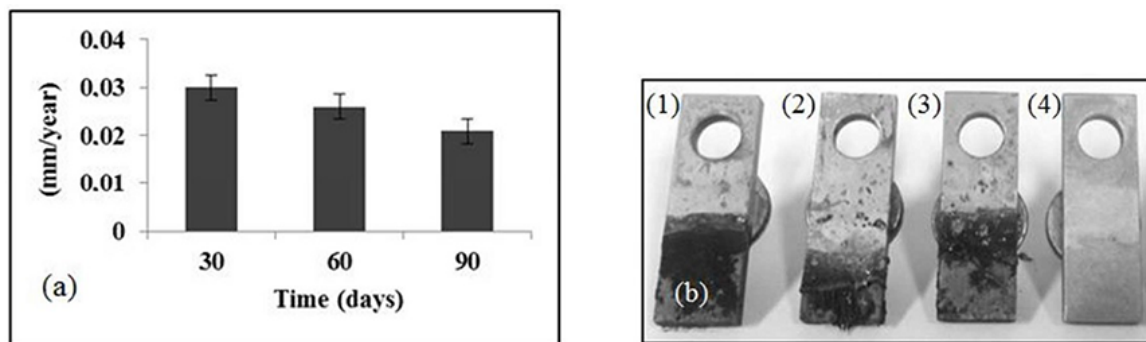


**Figure 4.** (a) Average corrosion rate of carbon steel ASTM A283 sample. (b) Samples immersed in oil/ water biphasic systems - (1) 30 days; (2) 60 days; (3) 90 days; (4) 90 days immersion in Diesel S10.

the more moisture in the fuel, the greater the chances that microorganisms will develop and, consequently, contribute to corrosive actions on the substrate<sup>19</sup>.

As observed in Fig. 4a, there was a reduction in the corrosion rate as a function of the immersion time, for the biphasic system. The highest corrosion rate was found at 30 days of immersion. During this period, the sample underwent accelerated corrosion due to direct exposure of the metal surface to the medium, which was initially free of a protective layer. Over time, deposits of solid particles, corrosion products and adhesion of microorganisms that promoted a physical barrier, thereby inhibiting the access of the electrolyte to the substrate, due to the protective layer on the surface, were observed (Figure 4b (1, 2, 3)). A relevant factor is that the physical-chemical analysis of the water revealed a low chloride concentration (as explained in item 3.1), which promoted a reduction of the aggressive effect of this medium<sup>18,20</sup>. Therefore, the corrosion rate was reduced due to lack of contact between the electrolyte and the metal, while the metal part was still immersed in a medium that presented low corrosivity.

Lopes et al.<sup>21</sup> reported that microorganism-induced corrosion in fuel storage tanks occurred due to the presence of water, which is a medium in which bacteria are present and abundant. To this extent, bacteria can migrate from one fluid to another, i.e., they can contaminate the diesel through the bacteria present in the water. This may cause corrosion on the surface of the metal in contact with the oil, given that surface exposure to localized attack can contribute to the loss of material.

### 3.3.2. Analysis of morphology and surface elements

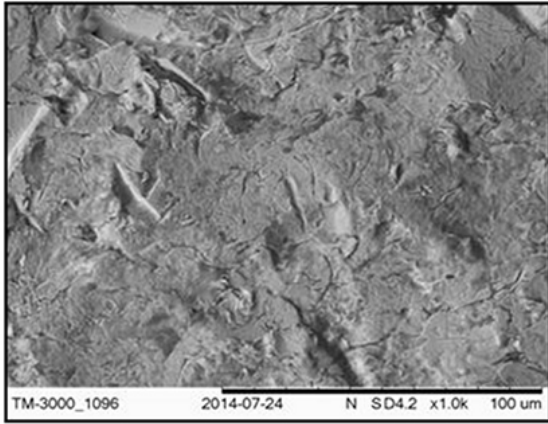
Fig. 5a shows the micrograph of the standard surface, performed before the immersion process. It was compared to the surface immersed in biphasic system after 60 days (Fig. 5b): diesel (region 1) / water (region 2). It was also compared to the surface immersed in Diesel S10 oil after 90 days (Fig. 5c). These results show the extent of deterioration of these surfaces after such immersion times.

The medium containing water presented high conductivity, thus providing an exchange of ions between the electrolyte and the substrate, leading to localized corrosion, as shown in region 2 of Fig. 5b. According to Vieira<sup>22</sup>, when the metal is immersed in water, corrosion is more aggressive initially because there are no protective layers on the surface of the metal. Corrosion products and biofilms have not yet formed at this early stage. Therefore, the speed with which the corrosion process is occurring is more intense. Over time, nonetheless, this layer that forms prevents the electrolyte from coming into direct contact with the substrate. Consequently, this protective layer favors a reduction in the corrosion process, in the following times, due to the formation of deposits that cause an increase in the resistance to the reaction of the corrosion.

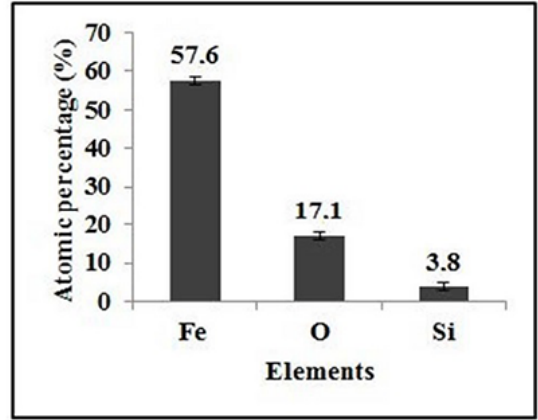
The results of the samples immersed in the system, containing Diesel S10 oil (Fig. 5c), show that localized corrosion occurred, although the corrosion rate was classified as low. This type of mechanism of corrosion can occur due to the action of acid metabolites generated by microorganisms present in the medium<sup>22</sup>. According to Rodrigues et al.<sup>23</sup>, the bacteria likely found in diesel oil are sulfate-reducing bacteria, fermenters, total anaerobic bacteria, total aerobic bacteria, iron-precipitating bacteria and fungi.

When doing a semiquantitative analysis of EDS, the presence of Fe, O and Si was detected, as shown in Fig. 5d. These are constituent elements of the ASTM A283 carbon steel composition and the Si may be sourced from the glass microspheres used during blasting or from Si compounds present in the fluid. The elements (Na, Ca, F) detected in the EDS of Figure 5 (e, f) are residual and are present in the water. Fluoride, on the other hand, is the residual present in the fuel, derived from the fluoranthene compound<sup>24</sup>, and, thus, its quantity becomes insignificant. Hence, the analysis of EDS only has a foundation when associated with XRD analysis, where the elements found in the semiquantitative analysis may suggest the presence of corrosion products in the phases found in XRD. Delaunoy et al.<sup>16</sup> observed generalized internal corrosion in steel tubes in systems containing water. EDS analysis on the surface of the pipe

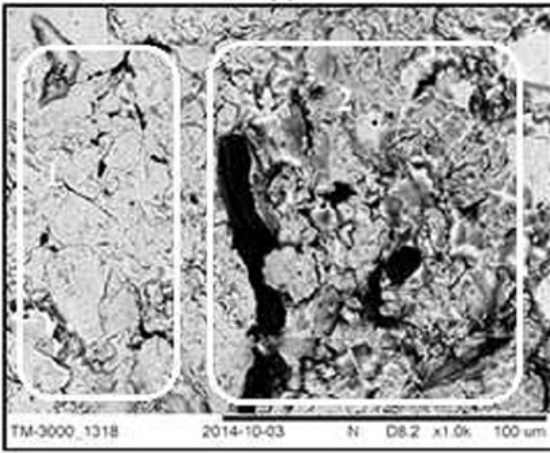




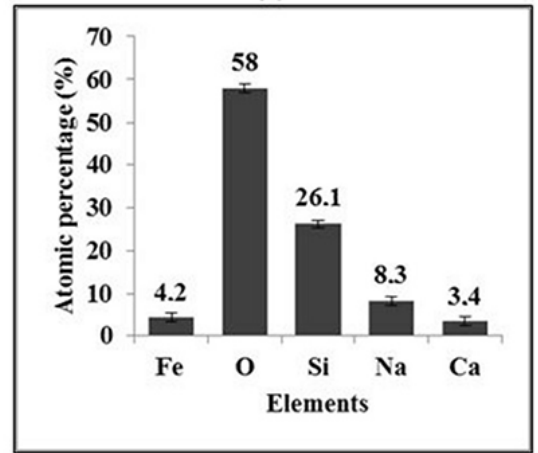
(a)



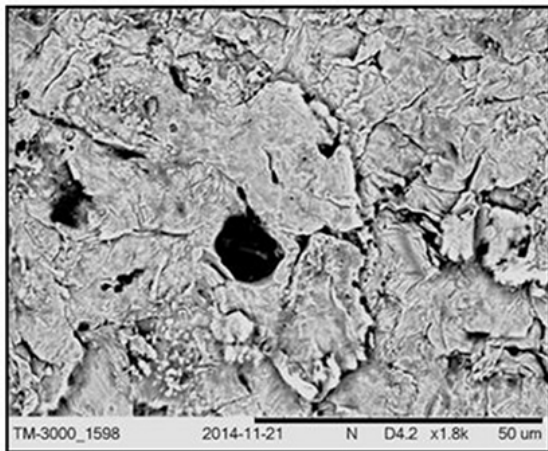
(d)



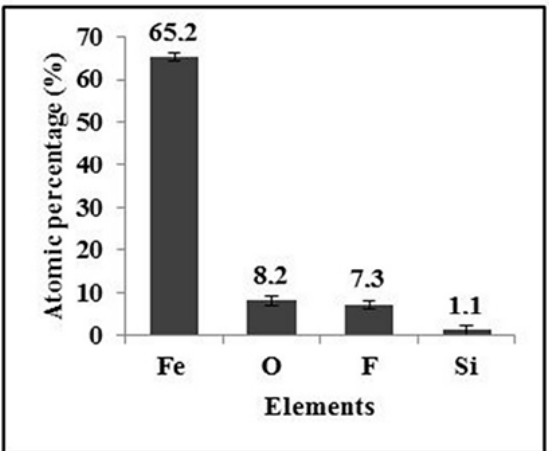
(b)



(e)



(c)



(f)

**Figure 5.** Micrographs. (a) Samples before starting the experiments; (b) Body immersed in biphasic system, in the region containing water, after 60 days of immersion; (c) Body immersed in pure diesel oil after 90 days of immersion; (d, e, f) respectively. Magnification: (a) 1000X; (b) 1000X; (c) 1800X.



**Figure 6.** SEM of the specimen exposed in the water-containing region, immersed in oil/water system after 60 days; Magnification: 20.000X.

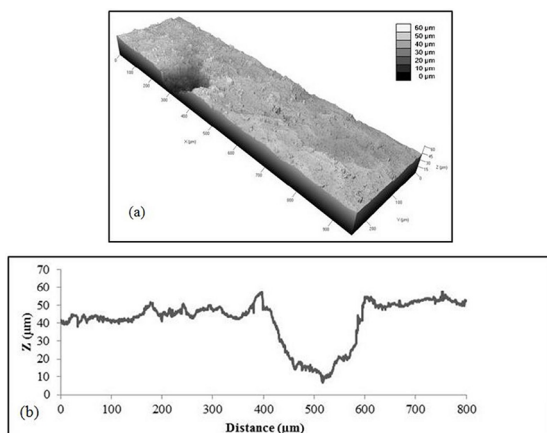


**Figure 7.** (a) Topography of the specimen, after 60 days of immersion in a two-phase system; (b) Roughness profile.

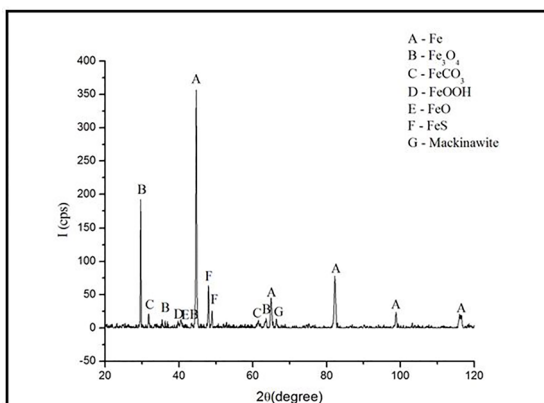


**Figure 8.** XRD spectrum of the metal surface, after 60 days of immersion in a biphasic system.

indicated Fe oxidation, due to the high percentage of oxygen, besides the presence of different elements of the chemical composition of the drinking water, such as: Cl, Ca, Si, P and Pb. According to Xu et al.<sup>20</sup>, the surface of the low-alloy steel, immersed in water, suffered less severe corrosion due to the formation of the  $\text{CaCO}_3$  layer, which protected the surface.

Fig. 6 shows the formation of the layer deposited in the sample for the biphasic diesel / water system for 60 days. The results showed superficial regions, which suggest they are products of corrosion (region 1) and extracellular polymeric material (EPM) (region 2), involving some isolated bacterial cells (region 3). The surface of the metal presented regions with a heterogeneous and irregular structure, due to the dynamism in the formation of the biofilm. This surface heterogeneity provided the presence of cavities and grooves that are characteristic of alveolar localized corrosion, resulting from the differential aeration mechanism (as will be seen in Fig 7a). Vieira<sup>18</sup> studied the occurrence of corrosion and biocorrosion in API 5L X60 steel, exposed to crude oil and water produced from 15 to 90 days of immersion. These results also showed deteriorated surfaces with the presence of cavities and furrows, in addition to new cells, that detach and adhere due to the dynamic way in which the biofilm formed and the corrosion products were generated, and also the presence of extracellular polymeric material and isolated bacterial cells. According to Oliveira<sup>25</sup>, in static systems, a thicker biofilm is formed, which presents a porous, non-compacted and non-adherent structure. This allows the electrolyte to reach the metal, due to the structure of the biofilm that forms irregularly or heterogeneously, over the surface. Therefore, there was a discrete loss of mass, indicating that, despite corrosion, it had no adverse effect on the useful life of the metal.

### 3.3.3. Influence of the corrosion process on the topography and roughness of the sample

Comparisons between the images of the standard surfaces and after 30, 60 and 90 days showed grooves or cavities that are characteristic of localized alveolar corrosion. Especially at 60 days, as shown in Fig. 7a. This type of corrosion showed a rounded bottom and a depth inferior to its diameter (Fig. 7b). According to Arruda<sup>26</sup>, the biofilm growth on rough surfaces promoted more niches for the adhesion of the microorganisms due to the greater contact area of the metal surface. Consequently, the biofilm grew thicker, with grooves protecting the bacteria that adhered to the surface of the forces that could remove them. Fig. 7b shows the graph of the roughness profile, with the formation of a large cavity, with a rounded bottom and a depth (50  $\mu\text{m}$ ) smaller than the diameter (200  $\mu\text{m}$ ), which suggests the presence of localized alveolar corrosion<sup>27</sup>. These variations caused changes in the

arithmetic mean of the roughness ( $R_a$ ) and the arithmetic mean of the surface roughness ( $R_{sa}$ ). Before the immersion process in a two-phase system and in a system containing the Diesel S10,  $R_a$  and  $R_{sa}$  values were 1.7  $\mu\text{m}$  and 2.3  $\mu\text{m}$ , respectively, for all specimens.

At 30 days of immersion the surface was not completely protected because the layer formed was very irregular or heterogeneous, thus generating a higher rate of corrosion during that period. Despite the corrosion, the roughness of the surface was practically unchanged after the cleaning process, and so maintained the same values of  $R_a$  (1.7  $\mu\text{m}$ ) and  $R_{sa}$  (2.3  $\mu\text{m}$ ).

At 60 days of immersion, localized corrosion was detected. The value for  $R_a$  was 9.1  $\mu\text{m}$  and  $R_{sa}$  was 3.6  $\mu\text{m}$ . These results are consistent with the formation of alveolar corrosion. The analysis of the roughness profile was performed exactly on the groove that had formed. Consequently, there was a sharp change in the result for  $R_a$ , as this analysis is more sensitive which comprises only a single profile, as shown in Fig. 7b. When analyzing the occurrence of this localized corrosion, it was observed that at 60 days, the results of the quantifications, in Fig. 3, showed a maximum growth of some bacteria, which boosted the corrosion process. Consequently, use of the XRD analysis (Fig. 8) led to it being found that there was a greater adhesion of the corrosion products during this period. Despite this protective layer, a localized corrosion process was observed after the cleaning process. Lee et al.<sup>28</sup> studied the influence of surface roughness on the corrosion resistance of steel to corrosion. The results showed that this resistance was closely related to the distribution of surface grooves, which affected the diffusion of active ions during corrosion, in specimens with rough surfaces. They found that the pitting formation occurred preferably aligned along the grooves and that surface roughness contributed to the localized corrosion process. Xu et al.<sup>20</sup> also analyzed corrosion products that adhered to the surface of low alloy carbon steel and detected iron (III) oxide-hydroxide (FeOOH). This layer separated from the surface and formed a film that was less adherent and had irregularities, which contributed to less protected regions being present, which led to the localized corrosion.

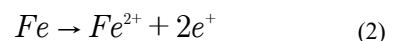
After 90 days of immersion in the biphasic system, by the kinetics of the biofilm itself, the layer was released, thereby creating unprotected regions, which increased surface roughness, in relation to the standard value, i.e., before the immersion process. Hence, the values of  $R_a$  and  $R_{sa}$  were 5.2 and 4.3. XRD analysis enabled this to be visualized as all the constituent species of the corrosion products that existed at 60 days were no longer detected.

At 90 days of immersion in a system containing only Diesel S10 Diesel, there were also no changes in surface roughness, which was evidenced by the low corrosion rate.

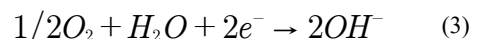
### 3.3.4. X-ray diffraction analysis (XRD)

Before starting the experiments, only Fe was detected, since the surface did not contain products of corrosion, given that the specimens had undergone the process of blasting and cleaning. After 30 days, the formation of phases indicative of oxides was observed, thus confirming that corrosion was occurring. On that account, the spectra presented, in addition to Fe, the formation of the compound of magnetite ( $\text{Fe}_3\text{O}_4$ ), siderite ( $\text{FeCO}_3$ ) and iron (III) oxide-hydroxide (FeOOH). This behavior is associated with the initial process, in which there is a layer consisting of corrosion products still in formation, which favors the detection of only a few phases. However, at 60 days of immersion, Fig. 8 showed that, in addition to these phases, new constituents of corrosion products were detected: iron oxide (FeO), iron sulphide (FeS) and the formation of the compound of iron sulphide which includes mackinawite ( $\text{Fe}_{1+x}\text{S}$ ). These new detected phases correspond to the protective layer that has developed. Since no sulfur was detected in the composition of this steel, (if detected it would be just a residual value, and would not be a significant value), probably the reactions occurred because of the presence of the sulfur present in the Diesel S10 oil and the sulfate found in the water. After 90 days of immersion, when this layer was removed from the surface, and also due to the biofilm renewal cycle, the results were the presence of only two compounds that indicate the corrosion process: iron (Fe) and magnetite ( $\text{Fe}_3\text{O}_4$ ). AlAbbas et al.<sup>29</sup> also detected as constituents of corrosion products: an iron sulphide compound that included mackinawite ( $\text{Fe}_{1+x}\text{S}$ ), another biogenetic iron sulfide (FeS), siderite ( $\text{FeCO}_3$ ) and iron (III) oxide-hydroxide (FeOOH). According to Edyvean<sup>30</sup>, the mackinawite layer formed as a result of the  $\text{H}_2\text{S}$  reactivity with the iron is not stable and may have been dissolved by the medium. Therefore, this protective film may have caused failures due to the disruption of microbial action, bulky growth and oxidation, thus contributing to localized corrosion. According to Enning et al.<sup>31</sup>, some microorganisms converted the lactate to acetate through pyruvate to produce  $\text{FeCO}_3$ . According to Sun et al.<sup>32</sup>, the corrosion product is formed by the ions resulting from the anodic and cathodic reactions, as shown in Eqs. 2 and 3, respectively:

- Anodic reaction:



- Cathodic reaction:





Fe<sup>2+</sup> ions reacted with OH<sup>-</sup> ions, forming Fe(OH)<sub>2</sub>, as shown in Eq. 4, for the corrosion product.



This insoluble product usually occurs in neutral or basic medium, which in the presence of oxygen in the solution led to the formation of Fe(OH)<sub>3</sub> and  $\gamma$ -FeOOH as shown in Eqs 5, 6 and 7:

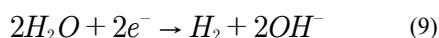


Also, in an oxygen deficient medium, there was the formation of magnetite (Eq. 8).

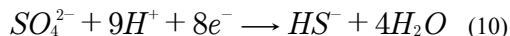


As for iron oxide, Fe<sub>2</sub>O<sub>3</sub>, when not hydrated, was in the form  $\alpha$ -Fe<sub>2</sub>O<sub>3</sub>, which is known as hematite, but when hydrated, its form was: Akaganeite ( $\beta$ -FeOOH), Lepidocrocite ( $\gamma$ -FeOOH) and Goetite ( $\alpha$ -FeOOH). Thus, rust can consist of three layers of hydrated iron oxides, in different oxidation states: FeO, Fe<sub>3</sub>O<sub>4</sub> e Fe<sub>2</sub>O<sub>3</sub>.

According to the metabolic activities of microorganisms, there is usually a cathodic reaction under depleted natural conditions (Eq. 9):



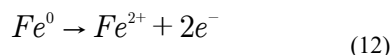
Thus, the microorganisms can use cathodic hydrogen to reduce sulfate to sulfide as follows (Eq. 10)<sup>33</sup>:



This reaction usually happens at a slow pace, with no bacteria biocatalysis. However, in systems containing microorganisms, the reaction can be rapid, being enzymatically catalyzed. Some hydrogen sulphide ions will convert to hydrogen sulphide, especially at acidic pH, as described in Eq. 11, below<sup>34</sup>:



The production of hydrogen sulphide and iron oxidation (anodic reaction) led to the formation of different types of iron sulphide as shown in Eqs. 12 and 13<sup>35</sup>:



According to Liu et al.<sup>36</sup> and Melo et al.<sup>37</sup>, the ferrous ions (Fe<sup>2+</sup>) produced by the dissolution process reacted with sulfide metabolised by the bacteria with the subsequent production of different forms of iron sulfide Fe<sub>y</sub>S<sub>x</sub> (Mackinwita, Jarosita, Pirotita and Greigita).

## 4. Conclusion

The corrosion behavior of the ASTM A283 carbon steel and the biodegradation of the Diesel S10 oil subjected to a biphasic immersion oil/water system were investigated and the following conclusions were obtained:

Corrosion and biocorrosion processes contributed to changes in chloride, iron and sulfate concentrations. These changes in the original composition of the medium may have occurred due to the microbial growth of the corrosion products and may also have been formed because of chemical reactions in the biphasic system.

When quantifying the microorganisms, the aerobic bacteria were active in the consumption of oxygen, which contributed to the development of the anaerobic bacteria. These microorganisms influenced the results of the corrosion rate on the metal surfaces.

The corrosion rate was classified as moderate for the specimens immersed in the biphasic system, and low for the specimens immersed in Diesel S10 oil. A decrease was observed in the corrosion rate during the 90 days of immersion in a two-phase system, which was associated to the formation of a layer consisting of corrosion products and biofilms throughout the experiments, which made it difficult for the electrolyte to reach the base metal.

SEM images showed localized corrosion and revealed biofilms, which adhered to the surface of the metal. Corrosion products have been found along with shapes that suggest that they are microbial cells that are involved in extracellular polymeric material.

Topographic analyzes confirmed the presence of localized alveolar corrosion in some regions, thus showing that corrosion did not occur generically and/or homogeneously. Moreover, the roughness of the surface contributed to accelerating the corrosion process and the formation of biofilms that adhered to the surface.

XRD spectra presented different phases, along with Fe as magnetite (Fe<sub>3</sub>O<sub>4</sub>), siderite (FeCO<sub>3</sub>), iron hydroxide oxide III (FeOOH), iron oxide (FeO) and iron sulphide, including FeS and (Fe<sub>x</sub>S<sub>y</sub>). These are constituents of the corrosion products, mainly after 60 days of immersion, which may be related to the mechanism of differential aeration.

## 5. Acknowledgements

We are grateful for the support to the develop this research study that we received from the Federal University of Pernambuco, Coordenação de Aperfeiçoamento de Pessoal de Nível Superior (CAPES), Conselho Nacional de Desenvolvimento Científico e Tecnológico (CNPq) and Fundação de Amparo à Ciência e Tecnologia de Pernambuco (FACEPE).

## 6. References

- Silva MVF, Pereira MCP, Codaro EN, Acciare HA. Carbon steel corrosion: an everyday approach to teaching chemistry. *Química Nova*. 2015;38(2):293-296.
- Brazil. Petrobras Distribuidora. *Manual Técnico Diesel S10*. Available from: <[http://sites.petrobras.com.br/minisite/assistenciatecnica/public/downloads/manual\\_tecnico\\_diesels-10\\_assistencia\\_tecnica\\_petrobras.pdf](http://sites.petrobras.com.br/minisite/assistenciatecnica/public/downloads/manual_tecnico_diesels-10_assistencia_tecnica_petrobras.pdf)>. Access in: 22/12/2017.
- Song X, Yang Y, Yu D, Lan G, Wang Z, Mou X. Studies on the impact of fluid flow on the microbial corrosion behavior of product oil pipelines. *Journal of Petroleum Science and Engineering*. 2016; 146: 803-812.
- Brazil. Agência Nacional do Petróleo, Gás Natural e Biocombustíveis (ANP). *Biocombustíveis*. Available from: <<http://www.anp.gov.br/wwwanp/biocombustiveis>>. Access in: 22/12/2017.
- Dias LC, Santos AR. Bacterial corrosion on tanks of kerosene and aviation gasoline. *UNISANTA - Science and Technology*. 2012;1(2):76-80.
- ASTM International. *ASTM A283/A283M - 13 - Standard Specification for Low and Intermediate Tensile Strength Carbon Steel Plates*. West Conshohocken: ASTM International; 2013.
- ASTM International. *ASTM G1-03(2011) - Standard Practice for Preparing, Cleaning, and Evaluating Corrosion Test Specimens*. West Conshohocken: ASTM International; 2011.
- NACE. *NACE RP-07-75 - Standard Recommended Practice - Preparation, Installation, Analysis and Interpretation of Corrosion Coupons in Oilfield Operations*. Houston: NACE; 2005.
- Penna MO, Baptista W, Brito RF, Nascimento JR, Silva ED, Coutinho CML. Dynamic system for the evaluation of CIM monitoring and control techniques. *Boletim Técnico da Petrobras*. 2002;45(1):26-33.
- American Public Health Association. *APHA Method 4110: Standard Methods for the Examination of Water and Wastewater*. Washington: American Public Health Association; 1992. Available from: &lt;<https://law.resource.org/pub/us/cfr/ibr/002/apha.method.4110.1992.pdf>&gt;. Access in: 08/01/2017.
- American Public Health Association. *APHA Method 3120: Standard Methods for the Examination of Water and Wastewater*. Washington: American Public Health Association; 1992. Available from: <<https://law.resource.org/pub/us/cfr/ibr/002/apha.method.3120.1992.pdf>>. Access in: 08/01/2017.
- Brazil. Agência Nacional do Petróleo, Gás Natural e Biocombustíveis (ANP). *Resolução ANP N° 50 de 23/12/2013*. Available from: <<https://www.legisweb.com.br/legislacao/?id=263587>>. Access in: 22/12/2017.
- Peters SR, Lima LRM, Silva SN, Rodrigues LM. Corrosão de aço carbono para dutos em águas naturais. In: *Proceedings of XI Congresso Brasileiro de Engenharia Química em Iniciação Científica*; 2015 Jul 19-22; Campinas, SP, Brazil . São Paulo: Blucher; 2015.
- Videla HA. *Biocorrosão, Biofouling e Biodeterioração de Materiais*. 1ª ed. São Paulo: Edgard Blücher; 2003.
- Su WT, Wu BS, Chen WJ. Characterization and biodegradation of motor oil by indigenous *Pseudomonas aeruginosa* and optimizing medium constituents. *Journal of Taiwan Institute of Chemical Engineers*. 2011;42(5):689-695.
- Delaunoy F, Tosar F, Vitry V. Corrosion behaviour and biocorrosion of galvanized steel water distribution systems. *Bioelectrochemistry*. 2014; 97:110-119.
- Lewandowski Z, Boltz JP. Biofilms in Water and Wastewater Treatment. In: Wilderer P, ed. *Treatise on Water Science. Volume 4*. Oxford: Academic Press; 2011. p. 529-570.
- Vieira MRS. Corrosion and biocorrosion in API 5L X60 steel exposed to crude oil and water produced. *Corrosão & Proteção*. 2012;9(44):20-27.
- Knothe G, Gerpen JV, Krahl J, Ramos LP. *Manual de Biodiesel*. 1ª ed. São Paulo: Edgard Blücher; 2006.
- Xu Q, Gao K, Wang Y, Pang X. Characterization of corrosion products formed on different surfaces of steel exposed to simulated groundwater solution. *Applied Surface Science*. 2015;345:10-17.
- Lopes FA, Morin P, Oliveira R, Melo LF. Interaction of *Desulfovibrio desulfuricans* biofilms with stainless steel surface and its impact on bacterial metabolism. *Journal of Applied Microbiology*. 2006;101(5):1087-1095.
- Vieira MRS. *Estudo dos processos de corrosão e biocorrosão causados por fluidos da indústria de petróleo*. [Thesis]. Recife: Federal University of Pernambuco; 2013.
- Rodrigues T, Oliveira A, Coutinho D, Guerreiro L, Galvão M, Souza P, et al. Diversity of microorganisms related to the biocorrosion in oil and gas systems. *Corrosão e Proteção de Materiais*. 2013;32(4):100-104.
- Birch ME, Cary RA. Elemental Carbon-Based Method for Monitoring Occupational Exposures to Particulate Diesel Exhaust. *Aerosol Science and Technology*. 1996;25(3):221-241.
- Oliveira SH. *Estudo da utilização de xantano e hipoclorito de sódio como estratégia para controlar a biocorrosão*. [Thesis]. Recife: Federal University of Pernambuco; 2010.
- Arruda EAF. *Estudo comparativo do processo corrosivo do aço patinável e do aço carbono comum*. [Monography]. Belém: Federal University of Pará; 2009.
- Gentil V. *Corrosão*. 6ª ed. Rio de Janeiro: LTC; 2011.
- Lee SM, Lee WG, Kim YH, Jang H. Surface roughness and the corrosion resistance of 21Cr ferritic stainless steel. *Corrosion Science*. 2012;63:404-409.
- AlAbbas FM, Williamson C, Bhola SM, Spear JR, Olson DL, Mishra B, et al. Microbial Corrosion in Linepipe Steel Under the Influence of a Sulfate-Reducing Consortium Isolated from an Oil Field. *Journal of Materials Engineering and Performance*. 2013;22(11):3517-3529.

30. Edyvean RGJ. Hydrogen sulphide - A corrosive metabolite. *International Biodeterioration*. 1991;27(2):109-120.
31. Enning D, Venzlaff H, Garrelfs J, Dinh HT, Meyer V, Mayrhofer K, et al. Marine sulfate-reducing bacteria cause serious corrosion of iron under electroconductive biogenic mineral crust. *Environmental Microbiology*. 2012;14(7):1772-1787.
32. Sun M, Xiao K, Dong CF, Li XG, Zhong P. Electrochemical behaviors of ultra-high strength steels with corrosion products. *Acta Metallurgica Sinica*. 2011;4:442-448.
33. Bholá R, Bholá SM, Mishra B, Olson DL. Microbiologically influenced corrosion and its mitigation (A review). *Materials Science Research India*. 2010;7(2):407-412.
34. Javaherdashti R. *Microbiologically Influenced Corrosion: An Engineering Insight*. London: Springer; 2008.
35. Cetin D, Aksu ML. Corrosion behavior of low-alloy steel in the presence of *Desulfotomaculum* sp. *Corrosion Science*. 2009;51(8):1584-1588.
36. Liu T, Liu H, Hu Y, Zhou L, Zheng B. Growth characteristics of thermophile sulfate-reducing bacteria and its effect on carbon steel. *Material and Corrosion*. 2009;60(3):218-224.
37. Melo IR, Urtiga Filho SL, Oliveira FJS, França FP. Formation of Biofilms and Biocorrosion on AISI-1020 Carbon Steel Exposed to Aqueous Systems Containing Different Concentrations of a Diesel/Biodiesel Mixture. *International Journal of Corrosion*. 2011;2011:415920.